Galleria mellonella larvae exhibit a weight-dependent lethal median dose when infected with Methicillin-resistant *Staphylococcus aureus*

Authors

Poppy J. Hesketh-Best[1*], Michelle V. Mouritzen[2], Kayleigh Shandley-Edwards[1], Richard A. Billington[1], and Mathew Upton[2]

[1]School of Biological and Marine Sciences, and [2]School of Biomedical Sciences, University of Plymouth, PL4 8AA UK.

* Corresponding author: Poppy J. Hesketh Best (poppy.heskethbest@plymouth.ac.uk)

Abstract

Galleria mellonella is a recognised model to study antimicrobial efficacy; however, standardisation across the scientific field and investigations of methodological components are needed. Here we investigate the impact of weight on mortality following infection with Methicillin-resistant *Staphylococcus aureus* (MRSA). Larvae were separated into six weight groups (180-300 mg at 20 mg intervals) and infected with a range of doses of MRSA to determine the 50% lethal dose (LD_{50}), and the 'lipid weight' of larvae post-infection was quantified. A model of LD_{50} values correlated with weight was developed. The LD_{50} values, as estimated by our model, were further tested *in vivo* to prove our model.

We establish a weight-dependent LD_{50} in larvae against MRSA and demonstrate that *G. mellonella* is a stable model within 180-260 mg. We present multiple linear models correlating weight with: LD_{50}, lipid weight, and larval length. We demonstrate that the lipid weight is reduced as a result of MRSA infection, identifying a potentially new measure in which to understand the immune response. Finally, we demonstrate that larval length can be a reasonable proxy for weight. Refining the methodologies in which to handle and design experiments involving *G. mellonella*, we can improve the reliability of this powerful model.

Key Words

Methicillin-resistant *Staphylococcus aureus*; *Galleria mellonella*; antibiotic testing; LD_{50}; pre-clinical model; fat body

Introduction

Galleria mellonella (Greater wax moth) larvae are widely utilised for toxicity screening (Desbois and Coote 2012; Maguire, Duggan and Kavanagh 2016; Coates *et al.* 2019) and to study host-pathogen interactions (Peleg *et al.* 2009; Olsen *et al.* 2011; Junqueira 2012; Wojda and Taszłow 2013). Unlike many insect models, *G. mellonella* can be incubated at 37°C, which facilitates the investigation of human pathogens. This has included most of the ESKAPE pathogens: *Enterococcus faecium* (Chibebe Junior *et al.* 2013; Luther *et al.* 2014); *Staphylococcus aureus* (Brackman *et al.* 2011; Ramarao, Nielsen-Leroux and Lereclus 2012; Sheehan, Dixon and Kavanagh 2019); *Klebsiella pneumoniae* (Wand *et al.* 2013; Diago-Navarro *et al.* 2014); *Acinetobacter baumannii* (Peleg *et al.* 2009); and *Pseudomonas aeruginosa* (Jander, Rahme and Ausubel 2000; Seed and Dennis 2008). Additionally, *Escherichia coli* (Leuko and Raivio 2012; Alghoribi *et al.* 2014; Jønsson *et al.* 2017; Guerrieri *et al.* 2019)*, Bulkholderia mallei* (Schell, Lipscomb and DeShazer 2008) and several fungi (Cotter, Doyle and Kavanagh 2000; Reeves *et al.* 2004; Mylonakis *et al.* 2005) have also been studied using *G. mellonella*. Crucially, a positive correlation between the virulence and immune responses between mammalian models and *G. mellonella* has been established for *P. aeruginosa* (Jander, Rahme and Ausubel 2000), *Cryptococcus neoformans* (Mylonakis *et al.* 2005), and *S. aureus* (Sheehan, Dixon and Kavanagh 2019)*,* demonstrating the powerful potential of this invertebrate model.

Antibiotic efficacy at dosages recommended for human use can be tested in *G. mellonella*, in addition to their toxicity correlating with toxicity observed in murine models (Ignasiak and Maxwell 2017). This has been shown with both natural and synthetic compounds (Gibreel and Upton 2013; Smitten *et al.* 2019), opening up the possibility of a rapid and cheap model for the early stages of discovery and development of natural and synthetic products, without the challenges of ethical approval, specialist training and the difficulties of using mice-models in early-stage drug development. Infections caused by antibiotic-resistant *S. aureus* are of global

concern and it is listed as a high priority pathogen for which new antibiotics are urgently needed (The World Health Organisation 2017). Methicillin-resistant *S. aureus* (MRSA) has been utilised with *G. mellonella* for the study of virulence (Mannala *et al.* 2018), pathogenicity (Ebner *et al.* 2016), antimicrobial efficacy of existing antimicrobials (Ba *et al.* 2015; Ferro *et al.* 2016), and for novel candidates (Gibreel and Upton 2013; Jacobs *et al.* 2013; Dong *et al.* 2017) (Table S1).

Despite the increased popularity of *G. mellonella*, there is much variability in method application (Andrea, Krogfelt and Jenssen 2019). This includes differences in larval size, storage, infective dose, and injection intervals. In this study, we address larval size and its potential impact in experimental design. In antibiotic efficacy studies, typically the model is infected with a pathogen shortly before the candidate treatment is presented. This has not been standardised with respect to the parameters previously mentioned for *G. mellonella*. In our preliminary experimentation in determining a 50% lethal dose (LD_{50}) for MRSA in *G. mellonella*, it was noted that smaller larvae were more susceptible to infection than larger larvae. This was when using a broad range of larval weights (~200-300 mg), as previously reported (Jacob*s et al*. 2013). Furthermore, the larval weight has been demonstrated to positively correlate with the larval liquid volume, leading to recommendations on how *in vivo* concentrations of injected compounds and pathogens should be calculated (Andrea, Krogfelt and Jenssen 2019). This led us to hypothesise that the larvae LD_{50} for a pathogen, in our case here MRSA, is directly proportional to the larvae weight and that larvae weight is an essential parameter in experimental design that must be tightly controlled.

When physical and anatomical barriers are breached, the wax moth larvae have an innate immune response relying on germline-encoded factors for the detection and clearance of microbial pathogens (Trevijano-Contador and Zaragoza 2019). There are two branches, cellular and humoral immunity. Cellular immunity is conducted by haemocytes, which are present in an open circulatory system called the haemolymph, which is analogous to vertebrate blood. There are at least six subpopulations of haemocytes which perform similar roles to those of the myeloid lineage in vertebrates (Boman and Hultmark 1987; Lavine and Strand 2002), and they are also associated with digestive system, trachea and fat body (Ratcliffe 1985). Five types of haemocytes were identified in fifth larval instar of *G. mellonella*;

prohaemocytes, plasmatocytes, granulocytes, oenocytoids and spherulocytes (Salem *et al.* 2014).The main immune processes include coagulation, phagocytosis and encapsulation (Tojo *et al.* 2000). Circulating haemocyte density increases during pathogenesis due to the release of suspended cells from the fat body (Tojo *et al.* 2000). Haemocyte density and subpopulation variations changes with time of exposure to pathogen and pathogen virulence (Arteaga Blanco *et al.* 2017).

Melanisation additionally occurs in the haemolymph, the process of melanin production resulting in the darkened appearance of the larvae (Tojo *et al.* 2000). The humoral branch is involved in the production of lytic enzymes (Vogel *et al.* 2011), and antimicrobial peptides (AMPs) that are active against bacterial pathogens (Cytryńska *et al.* 2007; Tsai, Loh and Proft 2016). These molecules are mostly produced by the larval 'fat body', analogous to the mammalian liver, and are released into the haemolymph (Zasloff 2002).

A proteomic investigation has shown *S. aureus* infections lead to an increase in production of proteins such as AMPs and peptidoglycan recognition proteins (Sheehan, Dixon and Kavanagh 2019). Critically, the same study identified similarities between *G. mellonella* and mammal immune response to *S. aureus* infections. What has not been investigated is the physiological change in *G. mellonella* lipid as a result of *S. aureus* infections. For this investigation, we were motivated to quantify the lipid weight, a proxy for the fat body, of the larvae to observe how the fat body might have been affected as a result of MRSA infection.

The aim of the work here is to investigate methodological adjustments which may improve the reproducibility and reliability of using pet-food grade *G. mellonella* as an experimental model. This was achieved by (i) examining the effect of larval weight on the LD_{50} to MRSA infection, and (ii) characterising physiological changes occurring to lipid weight as a result of the larval immune response to MRSA.

Materials and Methods

Cultivation of MRSA

A single colony of Methicillin-resistant *Staphylococcus aureus* (MRSA) NTCT 12493 was streaked onto fresh Luria broth (LB, Fischer Scientific, UK; Tryptone 10 g/L, yeast extract 5 g/L, and sodium chloride 10 g/L) solidified with 1.5% agar (Acros

Organics, UK) 24 h before experimentation. Single colonies were suspended in Dulbecco A Phosphate buffered saline (PBS, Oxoid UK) to a range of optical density (OD) read at 600 nm (Eppendorf BioPhotometer, Netherlands). These dilutions were OD_{600} = 0.1 - 1.0 in 0.1 increments. Viable cell counts were made of each dilution.

Determining a weight-based LD_{50} for Galleria mellonella *larvae*

Larvae were purchased commercially from Livefoods UK Ltd. (Somerset, UK; www.livefoods.co.uk). On receipt, larvae were individually weighed using an accurate scale and grouped into the following weight bands: 180-200, 201-220, 221-240, 241-260, 261-280, and 281-300 mg. Larvae were stored at 4°C for up to 7 days in the dark with no food and water. Healthy larvae were identified by a uniform cream colour, with no indications of melanisation such as spots or markings (Fig. 1A) (Li *et al.* 2018). Larvae were euthanised by chilling them at 4°C for 1 h, before freezing them at -20°C for a minimum of 24 h.

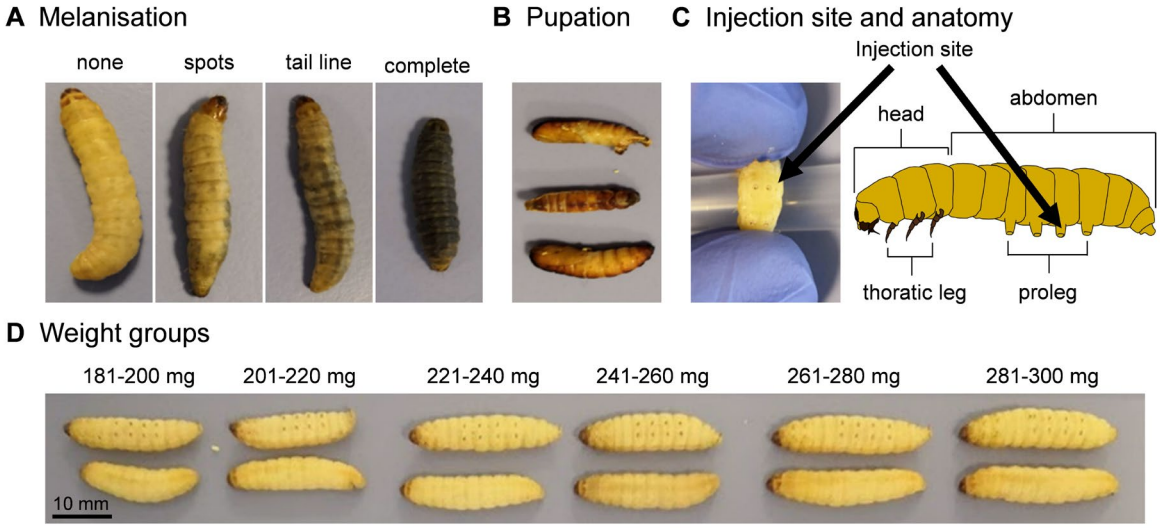

Figure 1: *Galleria mellonella* larvae. (A) Melanisation is a visual indication of the health of the larvae, as larvae progress from none to complete melanisation as a result of stress and/or infection. (B) Larvae pupation. (C) Route of infection for larvae is by intra-haemocoelic injection at the penultimate pro-leg (arrow). Larvae diagram was adapted from Singkum *et al.* (2019). (D) Larvae are divided up into six weight groups.

Larvae (n = 10) from each weight band were infected by injecting 10 µl of one of the 10 dilutions of MRSA into the left penultimate pro-leg (Fig. 1C), using a 50 µl Hamilton 750 syringe (Hamilton Company, UK) with a removable needle. Injected larvae were placed into Petri dishes lined with tissue paper (KIMTECH, UK). Three

independent replicates of this experiment were carried out. Syringes were cleaned before and after each bacterial dilution. Cleaning consisted of taking up and discarding of each wash solution thrice before progressing to the next wash solution. Wash solution order was as follows: distilled H_2O (dH_2O), 70% ethanol, and dH_2O.

After infection, the larvae were maintained at 37°C in the dark without food or water. A placebo control of sterile PBS was used to account for the effect of the physical trauma of injection, along with a non-manipulation (NM) control. After 24 h the live/dead counts were recorded. Larvae were recorded as dead when they met the following: (i) complete melanisation (Fig. 1A), (ii) did not respond to touch, and (iii) could not correct itself when rolled onto its back.

Determining the weight-dependent LD_{50}, live/dead counts were converted into percentage mortality at 24 h for each group. For this investigation we have defined LD_{50} as CFU of MRSA per mg of organism resulting in 50% mortality. To model the dose-response and describe the relationship between increasing the infection dose on survival for each weight group, a non-linear sigmoidal regression curve was plotted. The infection dose, represented as CFU/ mg of total weight of larva, was log-transformed. A non-linear regression curve was calculated to fit best the data generated from three independent replicas. From the equation generated from this curve, the theoretical LD_{50} was calculated along with the standard deviation (SD). Estimated LD_{50} from each weight groups were plotted against the mean larvae weight. A regression line was drawn, and the coefficient of determinant R^2 was calculated.

Correlating larval size with rate of pupation

On the day of receipt, larvae were placed into weight groups in Petri dishes. They were immediately placed at 37°C, in the dark with no food or water and permitted to pupate over 15 days. Larvae were observed daily and pupation events recorded.

Quantifying lipid weight of G. mellonella

Following investigation of the LD_{50} for MRSA, the lipid weight for all living and dead larvae was quantified. Live larvae from treatments, the NM and PBS controls were ethically euthanised. Dead larvae were stored at -20°C until needed. Larvae were left to thaw at room temperature for 24 h and were weighed and individually placed in

Eppendorf tubes to be dried over 7 days at 55°C, and re-weighed to reveal their dry weight. Larvae were then submerged in ≥99.9% diethyl ether (Sigma-Aldrich, UK) and left for 3 days at 4°C to dissolve lipid. Diethyl ether was utilised as the lipid extraction solvent (Tzompa-Sosa *et al.* 2014). After, ether was left to evaporate in a fume hood for 24 h. Once dried, larvae were weighed again to acquire the post-ether weight. Quantities are then presented as followed: 'total weight' is the weight of the larvae pre-experimentation; 'water weight' ($water\ weight = pre\text{-}experimentation\ weight\ -\ dry\ weight$); 'lipid weight' ($lipid\ weight = dry\ weight\ -\ post\text{-}ether\ weight$).

Statistical analysis

All statistical analysis was performed using PRISM GraphPad 8.4.2 (GraphPad Software, San Diego, CA, USA). One-Way ANOVA (two-tailed), Two-Way ANOVA, and Pearson's correlation coefficients were used when applicable to compare treatment groups. Log-rank Mantel-Cox tests compared survival curves for antimicrobial efficacy tests and pupation. A *p*-value of: < 0.05 ($*$), < 0.01 ($**$) or < 0.001 ($***$), < 0.0001 ($****$) was considered to be significantly different.

Results

Larval weight affects LD_{50}

To begin testing our hypothesis, LD_{50} values were determined for each weight group. A sigmoidal non-linear model best fit the dose-dependent response of the data, resulting in an LD_{50} calculated for each weight group (Fig. 2). When adjusted to the number of cells injected into each larvae per one unit of body weight (CFU/mg), the resulting LD_{50} ranged from 1.19 x10^7CFU/mg, for the 180-200 mg group, to the highest LD_{50} which was 8.97 x10^7 CFU/mg for the 261-280 mg group (Table 1). The LD_{50} increased across weight groups except for the 281-300 mg group, which had a lower LD_{50} than the 261-280 mg weight group. Throughout this experiment, we encountered some difficulties when handling larvae from the two higher weight-bands (261-280 and 281-300 mg), such as high variation in mortality at the lowest infective dosages (0-40% mortality) and highest dosages (60-100% mortality). Nevertheless, we were able to calculate an LD_{50} with the final data.

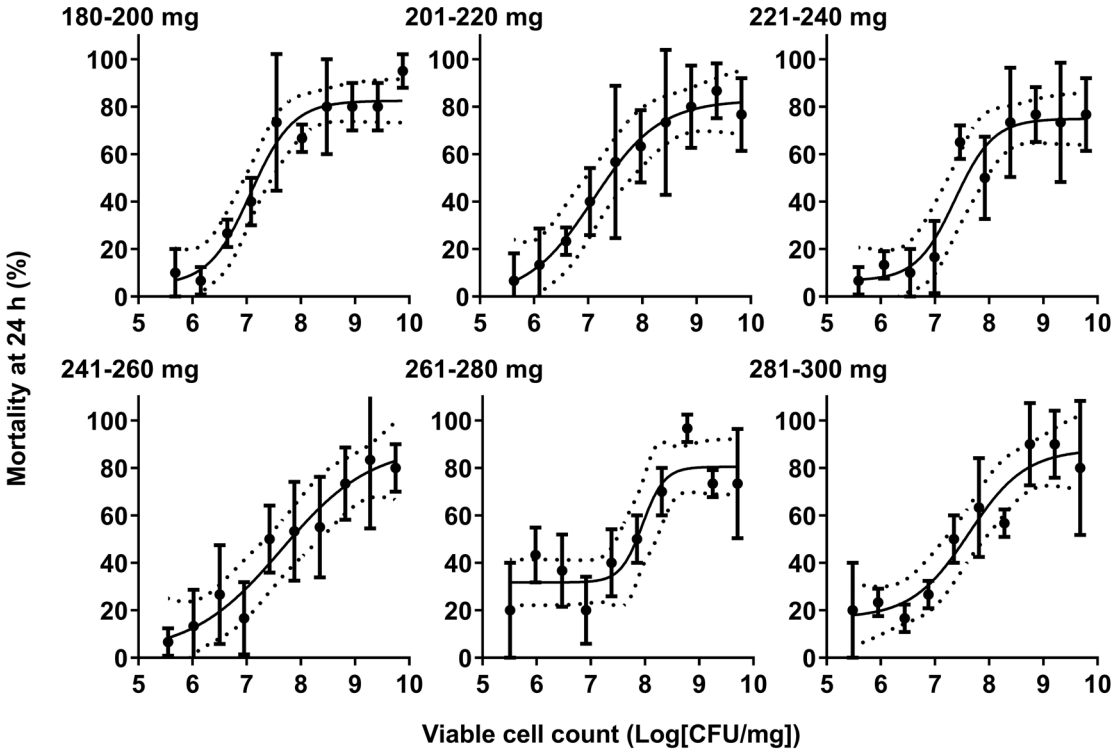

Figure 2. Sigmoidal non-linear logistic regressions best fit the dose-dependent response observed when calculating an LD_{50} for MRSA. LD_{50} was calculated for each weight group with 10 larvae/group. Data are shown as mean ± SD (n = 10) of three independent replicas.

Table 1. Summary of the LD_{50}s as calculated by non-linear models for each weight group (N, number of replicas; R^2, coefficient of determination).

Weight group (mg)	LD_{50} (CFU/mg)[(a)]	SD (CFU/mg)	N	R^2
180-200	1.19 x10^7	1.47	30	0.85
201-220	1.26 x10^7	2.45	30	0.77
221-240	2.34 x10^7	1.57	30	0.80
241-260	4.40 x10^7	3.35	30	0.76
261-280	8.97 x10^7	1.46	30	0.69
281-300	4.19 x10^7	1.81	30	0.78

[(a)]Example of how this is calculated can be found in Table S3

We observed a positive correlation between weight of the larvae and LD_{50}, as calculated by Pearson correlation test (r = 0.87, p = 0.025, n = 18). A linear regression model arriving at an equation ($y = 0.007966x + 5.548$) was used to estimate LD_{50} (Fig. 3A). The LD_{50} values, as estimated by our model, were tested *in*

vivo, demonstrating an approximate 50-56% (± 5.7 – 10%) survival for four of the weight groups (Fig. 3B). Survival at 24 h for the weight groups 261-280 and 281-300 mg was 30% (± 0%) and 43% (±15.3%), respectively.

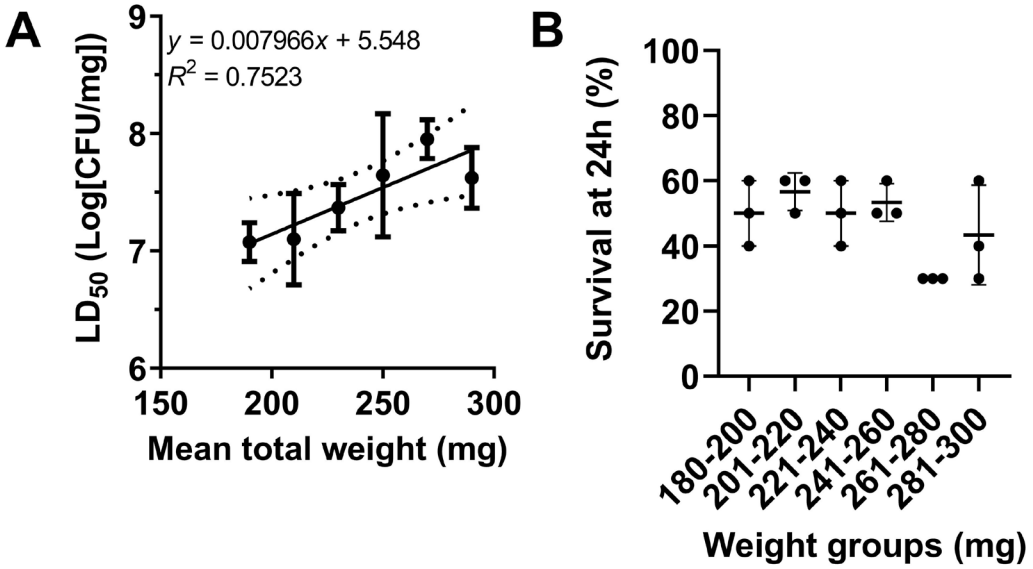

Figure 3. LD_{50} as calculated by non-linear regression models positively correlated with weight and was validated *in vivo* for all but the two highest weight groups. (A) Calculated LD_{50} by non-linear models correlation positively with total weight. (B) LD_{50} value as calculated by the model was validated by injecting into larvae and observing mortality. Data are shown as mean ± SD (n=10) of three independent replicas.

MRSA infection leads to a reduction in lipid weight

With the non-manipulated (NM) group, we assessed the overall relationship between total weight, dry weight, and lipid weight and length of the larvae (Fig. 4). Determined by Pearson's correlation test, we found a positive correlation between the total and dry weight, ($r = 0.972$, $p < 0.0001$, $n = 83$) (Fig. 4A), and total and water weight ($r = 0.989$, $p < 0.0001$, $n = 83$) (Fig. 4B). These two results support the findings of previous research (Andrea, Krogfelt and Jenssen 2019). Two additional positive correlations were observed between total weight and lipid ($r = 0.788$, $p < 0.0001$, $n = 83$) (Fig. 4C), and total weight and length ($r = 0.9944$, $p < 0.0001$, $n = 252$) (Fig. 4D).

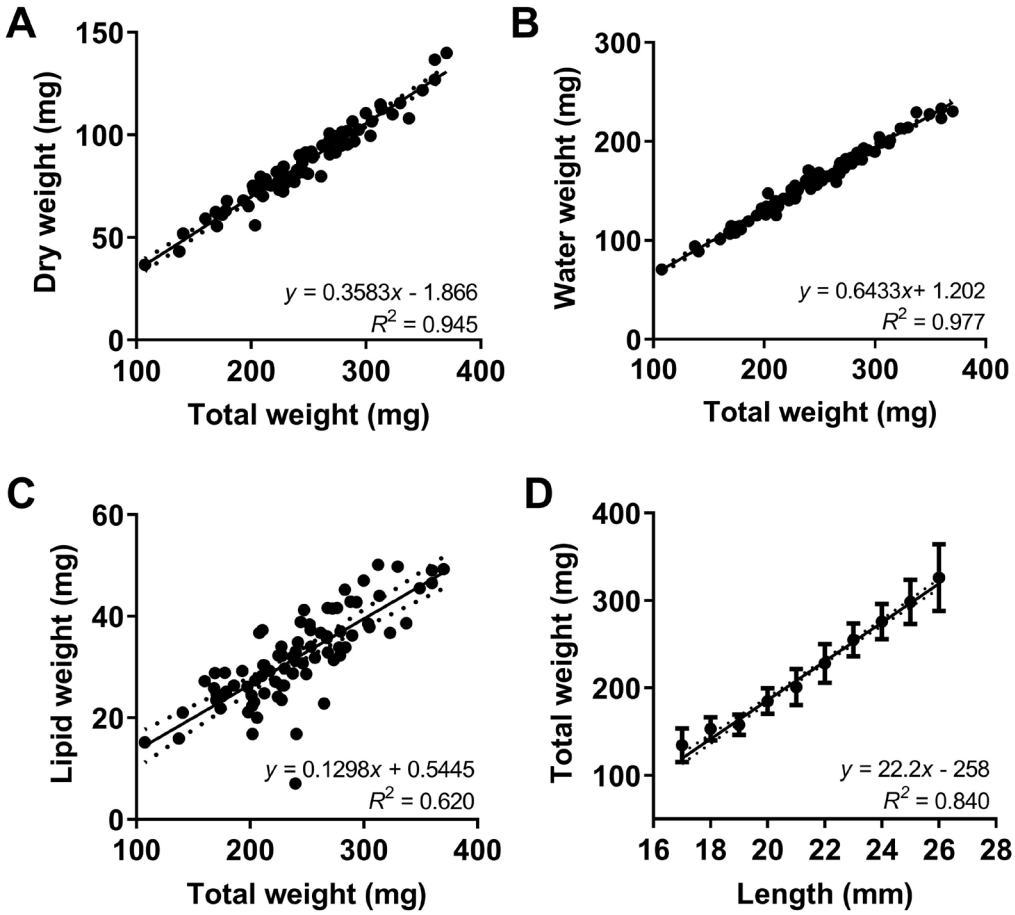

241

242 **Figure 4.** Multiple correlations observed between larvae total weight and dry weight, water
243 weight, lipid weight, and larvae length. Non-manipulated (NM) larvae were used to analyse
244 the relationships between (A) total weight and dry weight, (B) total weight and the lipid
245 weight after here presented as lipid weight, (C) total weight and lipid weight as proportional
246 to the total weight, water weight, and (D) total weight and larvae length where data is
247 presented as mean ± SD (n = 252).

248 We also investigated the effect of infection on the lipid weight of all the larvae used in
249 determining the LD_{50} for MRSA (Fig. 5). As calculated by one-way ANOVA, injection
250 with MRSA resulted in an overall decrease in the lipid weight for both dead (18.7 mg
251 ± 8.541, $p < 0.0001$, n = 573) and live larvae (22.4 mg ± 6.556, $p < 0.0001$, n = 524),
252 when compared to the NM control (31.92 mg ± 8.815, n = 83) (Fig 5A). When
253 compared to one another, live larvae had a significantly greater lipid weight
254 compared to dead larvae (p <0.0001). There was no significant reduction in the lipid
255 weight between NM and PBS control (27.81 mg ± 5.825, $p > 0.999$, n = 50) (Fig 5A
256 and Table S2).

257

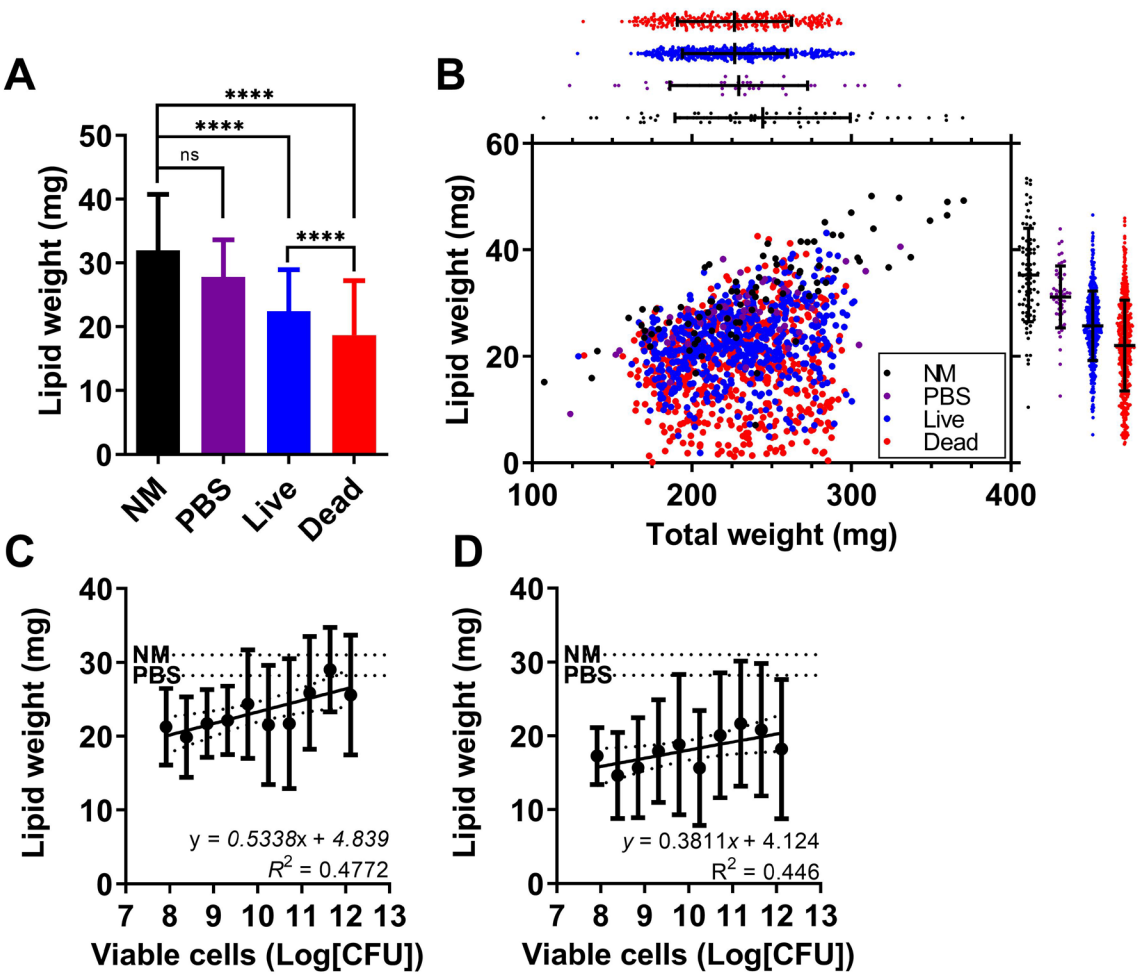

Figure 5. Injection of the larvae with MRSA results in an overall decreased in the lipid weight of the larvae. (A) Statistical results from a one-way ANOVA are illustrated above the bars as compared to the NM control. Summary of multiple analysis can be found in Table S2. (B) Box-plots above and to the right of the scatter plot are to illustrate the distribution of the data. Colours are as follows: black, NM control; purple, PBS control; blue, live larvae; and red, dead larvae 24 h post-MRSA infection. Correlations of infective dose and lipid weight for (C) living and (D) dead larvae. Data is presented as Log[CFU], as the infective doses are not adjusted for larvae weight. Data presented as mean ± SD (n = 10) of three independent replicas.

Finally, we observed that at a high infective dosage of MRSA, the larvae had a lipid weight close to the mean of the NM and PBS control compared to the lower dosages (Fig. 5C-D). This was supported by a positive correlation between lipid weight and infective dose for both live (r = 0.778, p = 0.008) (Fig. 5C) and dead larvae (r = 0.669, p = 0.035) (Fig. 5D).

Pupation is unaffected by weight

To explore whether larger larvae were closer to the final instar stage (pupae) in which they begin to pupate into adult moths, an observational experiment was performed. NM larvae were left to pupate at 37°C, and it was observed that 80-100% of larvae pupated within the 15 day incubation period, independent on their weight grouping, as calculated by Log-rank (Mantel-Cox) test ($X^2(5, N = 60) = 4.004$, $p = 0.549$) (Fig. 6).

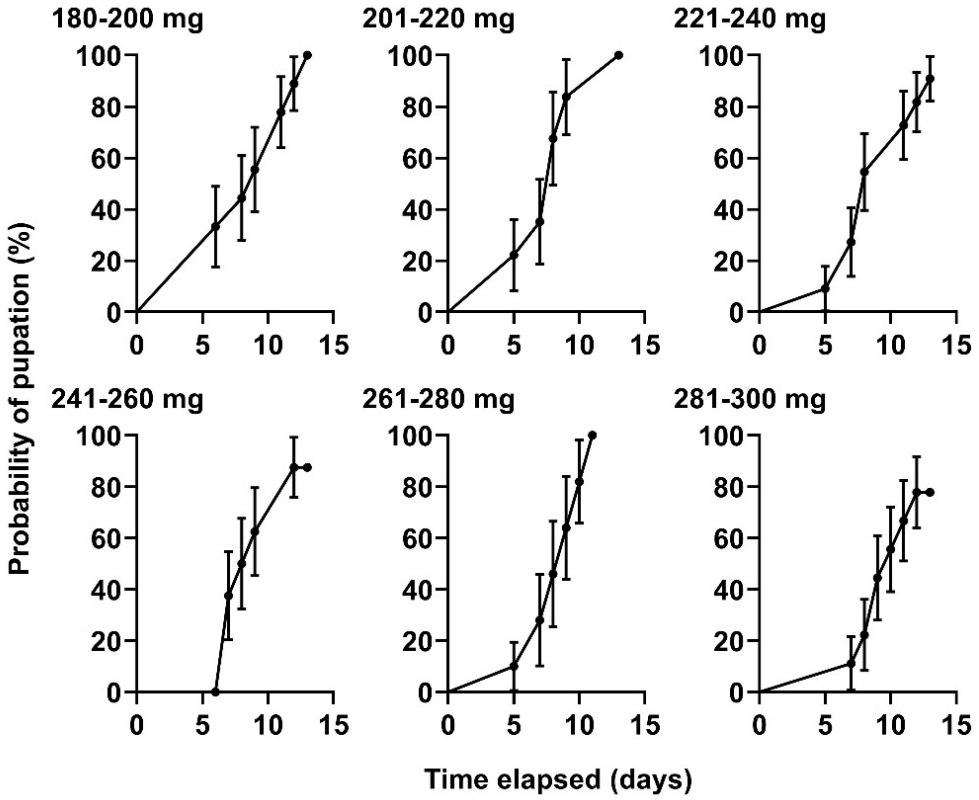

Figure 6. The weight did not influence the probability of pupation of NM larvae. NM larvae were incubated at 37ºC for 15 days and observed daily for pupation events. No significant difference was found between the weight group and the probability of pupation as calculated by a Log-rank Mantel-Cox test ($p = 0.5489$). Data are shown as mean ± SD (n = 10) repeated twice.

Discussion

MRSA exhibits a weight-dependent LD_{50}

In this study, we have demonstrated it is possible to develop a model in which a LD_{50} can be predicted based on the weight of the larvae, and that the prediction can be experimentally validated (Fig. 3). The linear model correlating total and water weight (Fig. 4B) imply that in increasingly larger larvae, the *in vivo* dilution of MRSA increases requiring a greater density of pathogen to reach the LD_{50}. Likewise for the

positive correlation confirmed with total and lipid weight (Fig. 4C), the presence of a larger fat body that can be degraded for the production of immune factors, may well be why we observe the weight-dependent effect on LD_{50}. The LD_{50}s (1.19 – 8.97 $x10^7$ CFU/mg) for the MRSA strain was not within range of infective dosages utilised in previously investigated MRSA and Methicillin-sensitive *S. aureus* (MSSA) strains (0.8 – 5.0 $x10^6$ CFU) (Table S1). However, a direct comparison may not be appropriate given the variation in reporting densities as in our study the LD_{50} was adjusted to account for *in vivo* dilution in the larvae as described in Andrea, Krogfelt and Jenssen (2019), but this is not always done.

During the process of this investigation, we found two of the largest weight groups (261-280 and 281-300 mg) to be unreliable, which hindered progress. This was consistent across multiple batches of larvae orders. LD_{50}, as calculated by our model for 261-280 and 281-300 mg larvae, resulted in less than 50% survival at 24 h (Fig. 3B), indicating that our model for a weight-dependent LD_{50} had overestimated the LD_{50}. Our first assumptions were that larger larvae were older and closer to pupation than the smaller weight groups, as larvae increase in size until pupation (Jorjão *et al.* 2018), which might somehow impact on survival. Given the difficulty in identifying an age for each larva, it is a difficult hypothesis to test beyond quantifying the number of days it took for NM larvae from each weight group to pupate.

When this was conducted, we found that larval size did not influence the probability of pupation (Fig. 6), and we conclude that the larvae received from the supplier had an 80-100% probability of pupating within 15 days if kept at 37°C, regardless of weight. It would appear that larger larvae were not likely to be closer to pupation than smaller ones, so the reason for our observed decrease in LD_{50} for large larvae remains unknown. Since larvae were kept without food, this may be a reason for the observed similar pupation times across all weight groups as lack of food source may be forcing the larvae into pupation. Feeding regimes are not the standard protocol when investing antibiotic efficacy, as such we feel this best represented the conditions larvae would be exposed to at the start of experimentation.

Using *G. mellonella* does have drawbacks, one such being the functional equivalent of adaptive immunity termed ‘immune priming’ (Little and Kraaijeveld 2004; Sadd and Schmid-Hempel 2006). Individual larvae that survive infection or exposure to a

particular pathogen may exhibit increased immune resistance against the same or similar pathogens. Priming with heat-killed pathogens was observed to result in increased larval survival (Wu *et al.* 2014). Ultimately there will be no control over the immune history of the larvae and this should always be recognised when working with pet-food grade *G. mellonella.* Across the literature, a wide range of weight bands have been utilised: 150-200 mg (Mannala *et al.* 2018); 300-700 mg (Ebner *et al.* 2016); 200-300 mg (Jacobs *et al.* 2013); and in other studies this is not declared (Ba *et al.* 2015; Jorjão *et al.* 2018). Our results suggest that choosing weight ranges as wide as 300-700 mg and 200-300 mg could result in inconsistent data. While a weight range of only 20 mg is likely a conservative approach, ranges such as 100 mg or greater in our weight-dependent LD_{50} model for MRSA indicates that there would be significant differences in survival (Fig. 3A).

Weighing individual larvae is a time-consuming procedure. This study also demonstrated that larvae length is reasonable proxy for the weight (Fig. 4D). Larval length has been previously used to characterise larvae for experimentation where larvae of 15-25 mm were utilised (Bazai*d et al*. 2018). Like total weight, a large length grouping may also encounter similar challenges. A 20 mg weight grouping would equate to roughly 1 mm, for example, 180-200 mg would be 20-21 mm. Measuring length may be a preferred alternative to accurately weighing all larval. When sourcing larvae from our supplier, we frequently found that larvae belonging to the weight groups 201-220 and 221-240 mg were most abundant, which will inevitably be the practical determining factor in weight group selection. Our findings would support selection of larvae in this range.

Lipid metabolism occurs in response to MRSA infection

MRSA infection leads to a decreased lipid weight in the larvae after 24 h, whether they died or survived the infection (Fig. 5A). The reduction in lipid weight is likely the result of lipolysis during an immune response. This is to be expected, the fat body of the larvae produce many defence compounds essential to the larvae's immune response (Cytryńska *et al.* 2007; Tsai, Loh and Proft 2016). This reaction can be rapid, in some models showing production of AMPs within the first 4 to 6 h post-infection (Sheehan, Dixon and Kavanagh 2019; Trevijano-Contador and Zaragoza 2019). This is supported by proteomic work, which demonstrated that at 6 and 24 h

post-*S. aureus* infection larvae had increased expression of AMPs (Sheehan, Dixon and Kavanagh 2019).

On exposure to the infecting pathogen, there may be a rapid metabolism of the fat body to provide the required energy to fight the infection. Larvae with larger lipid weight before infection might be more likely to survive, as seen with the surviving larvae having a greater lipid weight than dead larvae (Fig. 5A). Within this experimental design, the larvae are not fed before or during the experiment, and therefore they cannot be acquiring more lipid. Where lipid weight was seen as closer to the NM and PBS control baseline, as observed in the trend of lipid weight positively correlating with infective dose (Fig. 5C-D), it is more likely that lipid metabolism has been compromised.

What could reasonably be expected is that lipolysis of the fat body occurs to increase the production of AMPs and additional defence compounds. When *Drosophila* are stimulated by a systemic infection with *S. aureus*, signalling from the Toll receptor increases, which leads to increased production of AMPs and reduced accumulation of lipids (Liu *et al.* 2016; Lee and Lee 2018). This could suggest that for larvae surviving high infective dosages, there are additional immune responses that do not deplete the fat body.

We intended to quantify the larval lipid weight to aid in understanding the weight-dependent LD_{50} effect and the observed unreliability of the two largest weight groups (261-280 and 281-300 mg). We report several observations regarding the lipid weight and MRSA infection; however, none can fully explain the irregularity we encountered for the largest weight groups. Analysing larval lipid weight has proved some insight, but would benefit from further investigation, though alternative methods to estimate lipid mass would be required.

Overall assessment of G. mellonella *as a model*

There remains a lack of widely available and cheap standardised stocks of larvae reared under controlled conditions. Temperature (Mowlds and Kavanagh 2008), diet (Banville, Browne and Kavanagh 2012; Jorjão *et al.* 2018), past infections (Fallon, Kelly and Kavanagh 2012), and antibiotics and hormones in the feed (Büyükgüzel and Kalender 2008) are all reported to influence laboratory experimentation. Most

larvae currently used are acquired from commercial insect food providers (Andrea, Krogfelt and Jenssen 2019), where it is understood that use of antibiotics and hormones in the culture medium is common practice, and acquiring accurate information regarding the conditions in which the larvae are reared is challenging. All of which may vary between larvae suppliers, which is a challenge that warrants further investigation.

Ultimately from our investigation, it would appear that lipid deposits are essential in *G. mellonella* response to MRSA. Prior investigation has evaluated the effect of nutrient deprivation on larvae (Banville, Browne and Kavanagh 2012), and the selection of diet (Jorjão *et al.* 2018), which both influence susceptibility to *S. aureus* infection. This emphasises the issues associated with a having lack of knowledge of rearing conditions used by suppliers and how they will influence experimental results. TruLarv™ (BioSystems Technology, UK) currently provide the only standardised *G. mellonella* in the UK. While cheap compared to murine models, it is considerably costlier (£1.20 per larvae) than purchasing larvae from commercial pet food providers.

However for pet-food grade larvae to be reliably used in research, more significant consideration should be taken over the parameters that can be controlled, and in this study, we emphasise that such experiments can be reproducible and reliable. We recommend that investigators consider the potential variability associated with using different larval weight as we have shown herein. We would recommend using weight groupings as a means to control this. . Our data suggests that all larvae used should be within 10 mg of the mean weight of all larvae to provide consistency. Additionally, larvae of >260 mg should not be avoided.

In this work, we present several linear regression curves that could be used as tools to aid in experimental design, such as the linear model for LD_{50} (Fig. 3A), weight and lipid content (Fig. 4C), and length (Fig. 4D). Finally, we demonstrate that the lipid weight is reduced as a result of MRSA infection, identifying a potentially new measure in which to understand the immune response. Similarities between *G. mellonella* and mammals in response to *S. aureus* infections can be used to study the efficacy and interactions of novel antimicrobials, even at early development stages. By refining and standardising methodologies in which to handle and select

G. mellonella for study, we can improve the reliability of this powerful model for multiple purposes.

Author Contributions

Conceptualisation, PJHB and MVM; Methodology, PJHB, MVM, KSE, RAB, and MU; Validation, PJHB, MVM, and KSE; Formal Analysis, PJHB; Investigation, PJHB and MVM; Resources, PJHB and MVM; Data Curation, PJHB and MVM; Writing – Original Draft Preparation, PJHB; Writing – Review & Editing, PHB, MVM, KSE, RAB, and MU; Visualization, PJHB; Supervision, RAB, and MU; Funding Acquisition, MU.

Funding

This study was funded in part by the University of Plymouth, School of Biology and Marine Science postgraduate research studentship and Innovate UK Antibiotic Development grant (Innovate UK 103358).

Transparency declaration

The authors declare no conflict of interests. The funders had no role in the design of the study; in the collection, analyses, or interpretation of data; in the writing of the manuscript, or in the decision to publish the results.

References

Alghoribi MF, Gibreel TM, Dodgson AR *et al. Galleria mellonella* infection model demonstrates high lethality of ST69 and ST127 uropathogenic *E. coli*. *PLoS One* 2014;**9**:e101547–e101547.

Andrea A, Krogfelt KA, Jenssen H. Methods and Challenges of Using the Greater Wax Moth (*Galleria mellonella*) as a Model Organism in Antimicrobial Compound Discovery. *Microorganisms* 2019;**7**:85.

Arteaga Blanco LA, Crispim JS, Fernandes KM *et al.* Differential cellular immune response of *Galleria mellonella* to *Actinobacillus pleuropneumoniae*. *Cell Tissue Res* 2017;**370**:153–68.

Ba X, Harrison EM, Lovering AL *et al.* Old drugs to treat resistant bugs: Methicillin-resistant *Staphylococcus aureus* isolates with mecC are susceptible to a combination of penicillin and clavulanic acid. *Antimicrob Agents Chemother*

2015;**59**:7396–404.

Banville N, Browne N, Kavanagh K. Effect of nutrient deprivation on the susceptibility of *Galleria mellonella* larvae to infection. *Virulence* 2012;**3**:497.

Bazaid AS, Forbes S, Humphreys GJ *et al.* Fatty Acid Supplementation Reverses the Small Colony Variant Phenotype in Triclosan-Adapted *Staphylococcus aureus*: Genetic, Proteomic and Phenotypic Analyses. *Sci Rep* 2018;**8**, DOI: 10.1038/s41598-018-21925-6.

Boman HG, Hultmark D. Cell-free immunity in insects. *Annu Rev Microbiol* 1987;**41**:103–26.

Brackman G, Cos P, Maes L *et al.* Quorum sensing inhibitors increase the susceptibility of bacterial biofilms to antibiotics in vitro and in vivo. *Antimicrob Agents Chemother* 2011;**55**:2655–61.

Büyükgüzel E, Kalender Y. *Galleria mellonella* (L.) Survivorship, Development and Protein Content in Response to Dietary Antibiotics. *J Entomol Sci* 2008;**43**:27–40.

Chibebe Junior J, Fuchs BB, Sabino CP *et al.* Photodynamic and Antibiotic Therapy Impair the Pathogenesis of *Enterococcus faecium* in a Whole Animal Insect Model. *PLoS One* 2013;**8**:55926.

Coates CJ, Lim J, Harman K *et al.* The insect, *Galleria mellonella*, is a compatible model for evaluating the toxicology of okadaic acid. *Cell Biol Toxicol* 2019;**35**:219–32.

Cotter G, Doyle S, Kavanagh K. Development of an insect model for the in vivo pathogenicity testing of yeasts. *FEMS Immunol Med Microbiol* 2000;**27**:163–9.

Cytryńska M, Mak P, Zdybicka-Barabas A *et al.* Purification and characterization of eight peptides from *Galleria mellonella* immune hemolymph. *Peptides* 2007;**28**:533–46.

Desbois AP, Coote PJ. Chapter 2 - Utility of Greater Wax Moth Larva (*Galleria mellonella*) for Evaluating the Toxicity and Efficacy of New Antimicrobial Agents. In: Laskin AI, Sariaslani S, Gadd GM (eds.). *Advances in Applied Microbiology*. Vol 78. Academic Press, 2012, 25–53.

480 Diago-Navarro E, Chen L, Passet V *et al.* Carbapenem-resistant *Klebsiella*
481 *pneumoniae* exhibit variability in capsular polysaccharide and capsule
482 associated virulence traits. *J Infect Dis* 2014;**210**:803–13.

483 Dong CL, Li LX, Cui ZH *et al.* Synergistic effect of pleuromutilins with other
484 antimicrobial agents against *Staphylococcus aureus* in vitro and in an
485 experimental *Galleria mellonella* model. *Front Pharmacol* 2017;**8**:553.

486 Ebner P, Rinker J, Nguyen MT *et al.* Excreted cytoplasmic proteins contribute to
487 pathogenicity in *Staphylococcus aureus*. *Infect Immun* 2016;**84**:1672–81.

488 Fallon J, Kelly J, Kavanagh K. *Galleria mellonella* as a Model for Fungal
489 Pathogenicity Testing. *Methods Mol Biol* 2012;**845**:469–85.

490 Ferro TAF, Araújo JMM, dos Santos Pinto BL *et al.* Cinnamaldehyde Inhibits
491 *Staphylococcus aureus* Virulence Factors and Protects against Infection in a
492 *Galleria mellonella* Model. *Front Microbiol* 2016;**7**:2052.

493 Gibreel TM, Upton M. Synthetic epidermicin NI01 can protect *Galleria mellonella*
494 larvae from infection with *Staphylococcus aureus*. *J Antimicrob Chemother*
495 2013;**68**:2269–73.

496 Guerrieri CG, Pereira MF, Galdino ACM *et al.* Typical and Atypical
497 Enteroaggregative *Escherichia coli* Are Both Virulent in the *Galleria mellonella*
498 Model. *Front Microbiol* 2019;**10**:1791.

499 Ignasiak K, Maxwell A. *Galleria mellonella* (greater wax moth) larvae as a model for
500 antibiotic susceptibility testing and acute toxicity trials. *BMC Res Notes* 2017;**10**,
501 DOI: 10.1186/s13104-017-2757-8.

502 Jacobs AC, DiDone L, Jobson J *et al.* Adenylate kinase release as a high-
503 throughput-screening-compatible reporter of bacterial lysis for identification of
504 antibacterial agents. *Antimicrob Agents Chemother* 2013;**57**:26–36.

505 Jander G, Rahme LG, Ausubel FM. Positive correlation between virulence of
506 *Pseudomonas aeruginosa* mutants in mice and insects. *J Bacteriol*
507 2000;**182**:3843–5.

508 Jønsson R, Struve C, Jenssen H *et al.* The wax moth *Galleria mellonella* as a novel
509 model system to study Enteroaggregative *Escherichia coli* pathogenesis.

510 *Virulence* 2017;**8**:1894–9.

511 Jorjão AL, Oliveira LD, Scorzoni L *et al.* From moths to caterpillars: Ideal conditions
512 for *Galleria mellonella* rearing for in vivo microbiological studies. *Virulence*
513 2018;**9**:383–9.

514 Junqueira JC. *Galleria mellonella* as a model host for human pathogens: Recent
515 studies and new perspectives. *Virulence* 2012;**3**, DOI: 10.4161/viru.22493.

516 Lavine MD, Strand MR. Insect hemocytes and their role in immunity. *Insect*
517 *Biochemistry and Molecular Biology*. Vol 32. Pergamon, 2002, 1295–309.

518 Lee KA, Lee WJ. Immune–metabolic interactions during systemic and enteric
519 infection in *Drosophila*. *Curr Opin Insect Sci* 2018;**29**:21–6.

520 Leuko S, Raivio TL. Mutations that impact the enteropathogenic *Escherichia coli* Cpx
521 envelope stress response attenuate virulence in Galleria mellonella.
522 *Infect Immun* 2012;**80**:3077–85.

523 Li Y, Spiropoulos J, Cooley W *et al.* Galleria mellonella - a novel infection model for
524 the *Mycobacterium tuberculosis* complex. *Virulence* 2018;**9**:1126–37.

525 Little TJ, Kraaijeveld AR. Ecological and evolutionary implications of immunological
526 priming in invertebrates. *Trends Ecol Evol* 2004;**19**:58–60.

527 Liu B, Zheng Y, Yin F *et al.* Toll Receptor-Mediated Hippo Signaling Controls Innate
528 Immunity in *Drosophila*. *Cell* 2016;**164**:406–19.

529 Luther MK, Arvanitis M, Mylonakis E *et al.* Activity of daptomycin or linezolid in
530 combination with rifampin or gentamicin against biofilm-forming *Enterococcus*
531 *faecalis* or *E. faecium* in an in vitro pharmacodynamic model using simulated
532 endocardial vegetations and an *in vivo* sur. *Antimicrob Agents Chemother*
533 2014;**58**:4612–20.

534 Maguire R, Duggan O, Kavanagh K. Evaluation of *Galleria mellonella* larvae as an in
535 vivo model for assessing the relative toxicity of food preservative agents. *Cell*
536 *Biol Toxicol* 2016;**32**:209–16.

537 Mannala GK, Koettnitz J, Mohamed W *et al.* Whole-genome comparison of high and
538 low virulent *Staphylococcus aureus* isolates inducing implant-associated bone

539 infections. *Int J Med Microbiol* 2018;**308**:505–13.

540 Mowlds P, Kavanagh K. Effect of pre-incubation temperature on susceptibility of
541 *Galleria mellonella* larvae to infection by *Candida albicans*. *Mycopathologia*
542 2008;**165**:5–12.

543 Mylonakis E, Moreno R, El Khoury JB *et al. Galleria mellonella* as a model system to
544 study *Cryptococcus neoformans* pathogenesis. *Infect Immun* 2005;**73**:3842–50.

545 Olsen RJ, Ebru Watkins M, Cantu CC *et al.* Virulence of serotype M3 group A
546 *Streptococcus* strains in wax worms (*Galleria mellonella* larvae). *Virulence*
547 2011;**2**:111.

548 Peleg AY, Jara S, Monga D *et al. Galleria mellonella* as a model system to study
549 *Acinetobacter baumannii* pathogenesis and therapeutics. *Antimicrob Agents*
550 *Chemother* 2009;**53**:2605–9.

551 Ramarao N, Nielsen-Leroux C, Lereclus D. The insect *Galleria mellonella* as a
552 powerful infection model to investigate bacterial pathogenesis. *J Vis Exp* 2012,
553 DOI: 10.3791/4392.

554 Ratcliffe NA. Invertebrate immunity - A primer for the non-specialist. *Immunol Lett*
555 1985;**10**:253–70.

556 Reeves EP, Messina CGM, Doyle S *et al.* Correlation between gliotoxin production
557 and virulence of *Aspergillus fumigatus* in *Galleria mellonella*. *Mycopathologia*
558 2004;**158**:73–9.

559 Sadd BM, Schmid-Hempel P. Insect Immunity Shows Specificity in Protection upon
560 Secondary Pathogen Exposure. *Curr Biol* 2006;**16**:1206–10.

561 Salem HM, Hussein MA, Hafez SE *et al.* Ultrastructure changes in the haemocytes
562 of *Galleria mellonella* larvae treated with gamma irradiated *Steinernema*
563 *carpocapsae* BA2. *J Radiat Res Appl Sci* 2014;**7**:74–9.

564 Schell MA, Lipscomb L, DeShazer D. Comparative genomics and an insect model
565 rapidly identify novel virulence genes of *Burkholderia mallei*. *J Bacteriol*
566 2008;**190**:2306–13.

567 Seed KD, Dennis JJ. Development of *Galleria mellonella* as an alternative infection

model for the *Burkholderia cepacia* complex. *Infect Immun* 2008;**76**:1267–75.

Sheehan G, Dixon A, Kavanagh K. Utilization of *Galleria mellonella* larvae to characterize the development of *Staphylococcus aureus* infection. *Microbiol (United Kingdom)* 2019;**165**:863–75.

Singkum P, Suwanmanee S, Pumeesat P *et al.* A powerful in vivo alternative model in scientific research: *Galleria mellonella*. *Acta Microbiol Immunol Hung* 2019;**66**:31–55.

Smitten KL, Southam HM, de la Serna JB *et al.* Using Nanoscopy To Probe the Biological Activity of Antimicrobial Leads That Display Potent Activity against Pathogenic, Multidrug Resistant, Gram-Negative Bacteria. *ACS Nano* 2019;**13**:5133–46.

The World Health Organisation. *Global Priority List of Antibiotic-Resistant Bacteria to Guide Research, Discovery, and Development of New Antibiotics*., 2017.

Tojo S, Naganuma F, Arakawa K *et al.* Involvement of both granular cells and plasmatocytes in phagocytic reactions in the greater wax moth, *Galleria mellonella*. *J Insect Physiol* 2000;**46**:1129–35.

Trevijano-Contador N, Zaragoza O. Immune response of *Galleria mellonella* against human fungal pathogens. *J Fungi* 2019;**5**, DOI: 10.3390/jof5010003.

Tsai CJ-YY, Loh JMS, Proft T. *Galleria mellonella* infection models for the study of bacterial diseases and for antimicrobial drug testing. *Virulence* 2016;**7**:214–29.

Tzompa-Sosa DA, Yi L, van Valenberg HJF *et al.* Insect lipid profile: Aqueous versus organic solvent-based extraction methods. *Food Res Int* 2014;**62**:1087–94.

Vogel H, Altincicek B, Glöckner G *et al.* A comprehensive transcriptome and immune-gene repertoire of the lepidopteran model host *Galleria mellonella*. *BMC Genomics* 2011;**12**, DOI: 10.1186/1471-2164-12-308.

Wand ME, McCowen JWI, Nugent PG *et al.* Complex interactions of *Klebsiella pneumoniae* with the host immune system in a *Galleria mellonella* infection model. *J Med Microbiol* 2013;**62**:1790–8.

Wojda I, Taszłow P. Heat shock affects host-pathogen interaction in *Galleria*

mellonella infected with *Bacillus thuringiensis*. *J Insect Physiol* 2013;**59**:894–905.

Wu G, Zhao Z, Liu C *et al.* Priming *Galleria mellonella* (Lepidoptera: Pyralidae) Larvae With Heat-Killed Bacterial Cells Induced an Enhanced Immune Protection Against *Photorhabdus luminescens* TT01 and the Role of Innate Immunity in the Process. *J Econ Entomol* 2014;**107**:559–69.

Zasloff M. Antimicrobial peptides of multicellular organisms. *Nature* 2002;**415**:389–95.

Supplementary

Table S1. Summary of experimental design utilised for *G. mellonella* experiments. Table adapted from Andrea, Krogfelt and Jenssen (2019) to include details of strains and a brief summary of their characteristics. (LP, left pro-leg; NA, not available, P-, privately purchased larvae from country specified).

***S. aureus* strain**	**Strain characteristics**	**Larval weight/size**	**Larval origin**	**Storage**	**Injection site**	**Infection**	**Reference**
EDCC 5455-5461	clinical isolates	150–200 mg	Reared	30°C	Not given	1.0 x10^6	(Mannala *et al.* 2018)
EDCC 5464	clinical isolate, MRSA strain						
RN4220		NA	P-UK	4°C	Between segments	~1.3 x10^6	(Ba *et al.* 2015)
LGA251	veterinary isolate, *mecC* positive						
02.5099.D	clinical isolate, *mec*C positive						
ATCC 43300	MRSA, type culture	15–25 mm long	P-UK	7 days	LP	0.8–2.6 x10^6	(Bazaid *et al.* 2018)
Newman							
NCTC 13277	MRSA, type culture						
2x clin. isol.							
ATCC 29213	MSSA	~250 mg	P-China	NA	LP	~1.0 x10^6	(Dong *et al.* 2017)
ATCC 43300	MRSA						
N54	MSSA, clinical isolate						
MRSA N9	MRSA, clinical isolate						
USA300 JE2	MRSA	300–700 mg	P-Netherlands	NA	LP	1.0 x10^6	(Ebner *et al.* 2016)
ATCC 25923	type culture	~200 mg	NA	NA	LP	1.0 x10^3	(Ferro *et al.* 2016)
ATCC 6538	type culture						
SA01-04	clinical isolates						
USA300-0114		200–300 mg	P-USA	4°C, 14 days	LP	5.0 x10^6	(Jacobs *et al.* 2013)
UAMS-1							
UAMS-1112							
RN4220							
ATCC 6538	type culture	NA	Reared	28°C	NA	10^8 CFU/ml	(Jorjão *et al.* 2018)
ATCC 11195	MSSA, type culture	NA	P-UK	4°C, 14 days	NS	~2.5 x10^6	(Gibreel and Upton 2013)

Table S2. Multiple comparison results for change in lipid weight 24 h post-MRSA infection described in Figure 5. (PBS; phosphate-buffered saline injection; NM, no manipulation control)

Interaction	Mean rank diff.	Adjusted *p*-value	Summary
NM vs. PBS	78.87	>0.9999	ns
NM vs. Live	339.5	<0.0001	****
NM vs. Dead	490.7	<0.0001	****
PBS vs. Live	260.6	<0.0001	****
PBS vs. Dead	411.8	<0.0001	****
Live vs. Dead	151.2	<0.0001	****

Table S3. Editable excel table that can be used in order to calculate the LD50 for MRSA based on weight-grouping.

Calculating the LD50 for MRSA NCTC 12493

Equation as given by linear model: **y = 0.007966x + 5.548**

Larvae weight (mg): **x =**	*180*	*Insert here the median weight for the selected weight group*
LD_{50} (Log[CFU/mg]): **y =**	**9.61E+06**	This is the LD_{50} for your selected weight group
LD_{50} (CFU):	**2.88E+09**	This is the total density of MRSA 12493 that must be injected into larva of the selected weight-group in order to kill 50% of the population